ICSV13 - Vienna
The Thirteenth International Congress on Sound and Vibration
Vienna, Austria, July 2-6, 2006

MULTI-MODE SOUND PROPAGATION IN POD SILENCERS

Ray Kirby

School of Engineering and Design, Mechanical Engineering, Brunel University,
Uxbridge, Middlesex, UB8 3PH, United Kingdom
ray.kirby@brunel.ac.uk

Abstract

Pod silencers are dissipative silencers used in HVAC applications in which the absorptive material is used to line the outer wall of the duct and a central cylindrical pod is inserted to form a silencer with an annular flow passage. Pod silencers are used in a wide range of ductwork, from the relatively small to very large applications with duct diameters of the order of several metres, and so in general silencer performance is likely to be influenced by higher order mode propagation. Accordingly, a numerical mode matching technique is used here to model higher order mode propagation in a pod silencer. A comparison of predictions with those previously found assuming plane wave propagation is presented and it is demonstrated that, even for relatively small silencers, higher order modes play an important role in the performance of pod silencers.

INTRODUCTION

The cross-sectional shape of HVAC ductwork is typically rectangular, circular or flat oval. Dissipative silencers are used within this HVAC ductwork to attenuate broad-band noise emanating from a fan, although the silencers themselves tend to be restricted to rectangular or circular geometries. Rectangular dissipative silencers are normally fabricated using a series of parallel baffles, at least one of which is placed centrally in the duct to act as a "splitter". These central splitters are known to increase sound attenuation over and above that which may be expected simply by lining the walls of the duct. For a circular duct the same principle is adopted, only here the splitter is formed from a central cylindrical "pod" so that the silencer creates an annular flow passage. Thus, the design of pod silencers shares many similarities with the design of rectangular splitter silencers and one should account for sound

propagation inside the central pod as well as the lining on the wall. Moreover, both types of silencer are often used in applications in which the outer dimension of the duct varies from the relatively small to the very large, sometimes of the order of several metres. Thus, for medium to high frequencies, it is likely that the performance of rectangular splitter silencers and circular pod silencers will depend upon the propagation, and attenuation, of higher order modes. Accordingly, this article will focus on quantifying sound attenuation in cylindrical pod silencers by including higher order modes in the model, and also accounting for modal scattering over the inlet/outlet planes of the silencer.

Modelling relatively large dissipative silencers (e.g. over 1 m in diameter) is a challenge largely because of the size of the problem (either numerical or analytic). Normally, the silencer geometries are straightforward, however analytic techniques typically require a large number of modes before convergence is satisfactory, and numerical techniques require a large number of degrees of freedom. To overcome these problems a number of approaches have found favour. Traditionally, it has been common simply to compute modal attenuation rates in an equivalent infinite silencer, see for example [1] and [2] who examined rectangular splitter silencers; however, this method does not account for modal scattering at the inlet/outlet planes, which is known to be significant for most splitter silencers. Alternatively, Munjal [3] showed it is possible to model a finite length cylindrical pod silencer by limiting the analysis to plane wave propagation. Of course it is unlikely, given the typical range of applications of pod silencers, that Munjal's method will be accurate over a wide frequency range, especially in view of the influence of higher order modes in predictions obtained for large rectangular splitter silencers; see [4, 5, 6]. Thus, if one is to model accurately the performance of pod silencers then higher order propagating modes should be accounted for, in addition to modal scattering at either end of the silencer.

This article adopts a numerical mode matching approach, similar to the one described by Kirby [5], to model sound propagation in a large cylindrical pod silencer. Included in the model is the effect of a perforated sheet separating the absorbing material from the airway and an impervious fairing fixed to the inlet/outlet plane of the silencer. Transmission loss predictions are presented for two silencer geometries in the absence of mean flow.

THEORY

The geometry of the pod silencer is shown in Fig. 1, in which a multi-mode sound field is assumed to exist upstream of the silencer. The analysis proceeds by assuming that the acoustic fields in the inlet/outlet ducts, and also the silencer section, may be expanded as an infinite sum over the duct/silencer eigenmodes. On finding the duct/silencer eigenmodes, the modal amplitudes are computed by application of appropriate axial matching conditions (after suitable truncation of each modal sum).

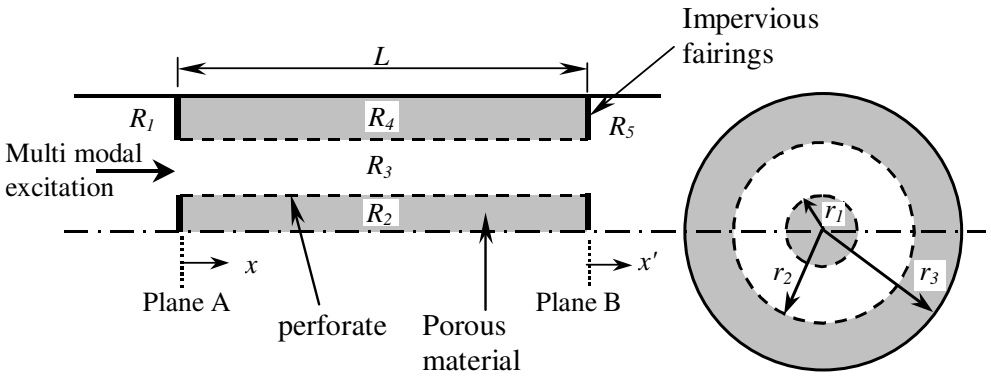

Figure 1. Geometry of pod silencer

A numerical approach, similar to that reported by Kirby [5], is adopted here so that a finite element eigenvalue analysis is followed by a point collocation scheme that fulfils the appropriate axial matching conditions. Accordingly, the acoustic wave equation is given as

$$\frac{1}{c_R^2}\frac{D^2 p_R'}{Dt^2} - \nabla^2 p_R' = 0\,, \tag{1}$$

where p_R' is the acoustic pressure in region R (where $R = 1,\ 2,\ 3,\ 4$ or 5), c_R is the speed of sound in region R and t is time. The acoustic field in each region is expanded as an infinite sum over the duct eigenmodes to give:

$$p_1'(x,r;t) = \sum_{j=0}^{\infty} F_j \Phi_j(r) e^{\mathrm{i}(\omega t - k_0 \gamma_j x)} + \sum_{j=0}^{\infty} A_j \Phi_j(r) e^{\mathrm{i}(\omega t + k_0 \gamma_j x)}\,, \tag{2}$$

$$p_c'(x,r;t) = \sum_{m=0}^{\infty} B_m \Psi_m(r) e^{\mathrm{i}(\omega t - k_0 \lambda_m x)} + \sum_{j=0}^{\infty} C_m \Psi_m(r) e^{\mathrm{i}(\omega t + k_0 \lambda_m x)}\,, \tag{3}$$

$$p_4'(x',r;t) = \sum_{n=0}^{\infty} D_n \Phi_n(r) e^{\mathrm{i}(\omega t - k_0 \gamma_n x')}\,. \tag{4}$$

Here, p_c' is the acoustic pressure in the silencer section; A_j, B_m, C_m, D_n and F_j are the modal amplitudes, λ_m is the (coupled) wave number for the silencer section, and γ_j is the wavenumber in the inlet/outlet section. The quantities $\Phi_j(r)$ and $\Psi_m(r)$ are the transverse duct eigenfunctions in the inlet/outlet region and the silencer section, respectively. In addition, $\mathrm{i} = \sqrt{-1}$ and $k_0 = \omega / c_0$, where c_0 is the isentropic speed of sound in air and ω is the radian frequency.

The task now is to solve the eigenvalue problem for the inlet/outlet ducts and

for the silencer section. The former problem is straightforward, whilst the latter problem has been discussed elsewhere ([4] and [5]), albeit for a rectangular geometry. For a circular geometry the analysis may take advantage of duct symmetry to model only one transverse dimension and so the following boundary conditions apply: (i) zero normal acoustic particle velocity at the wall, $r = r_3$; (ii) continuity of normal particle velocity over each perforate; and (iii) a pressure condition over each perforate. After discretising the silencer using a one-dimensional finite element mesh, and applying the transverse boundary conditions, a standard eigenvalue problem follows in terms of matrices [**A**] and [**B**] that may be found using the method of Kirby [5], where

$$[\mathbf{A}]\{\boldsymbol{\Psi}\} - \lambda^2 [\mathbf{B}]\{\boldsymbol{\Psi}\} = [\mathbf{0}]. \tag{5}$$

Equation (5) yields the silencer eigenvalues λ, and associated eigenvectors $\boldsymbol{\Psi}$. It is convenient to carry out the eigenvalue analysis for the inlet/outlet ducts using the same finite element mesh as for the silencer and then to enforce matching conditions over these common nodal locations. However, the addition of a perforate complicates matters, as additional nodes in the transverse finite element mesh are required at each perforate location in the silencer section. The solution lies in placing the additional nodes in the silencer section within the porous material, so that these nodes are not used when matching between the silencer and the inlet/outlet ducts [5].

Point collocation proceeds by matching across the inlet/outlet planes and enforcing the following matching conditions: for the airway (region R_3), continuity of pressure and particle velocity over planes A and B; for regions R_2 and R_4, zero normal particle velocity over each fairing. This yields eight coupled equations:

$$\sum_{j=0}^{N_1} A_j \boldsymbol{\Phi}_{3j} - \sum_{m=0}^{N_c} B_m \boldsymbol{\Psi}_{3m} - \sum_{m=0}^{N_c} \tilde{C}_m \boldsymbol{\Psi}_{3m} e^{-\mathrm{i}k_0 \lambda_m L} = -\sum_{j=0}^{N_1} F_j \boldsymbol{\Phi}_{3j}, \tag{6}$$

$$\sum_{j=0}^{N_1} A_j \gamma_j \boldsymbol{\Phi}_{3j} + \sum_{m=0}^{N_c} B_m \lambda_m \boldsymbol{\Psi}_{3m} - \sum_{m=0}^{N_c} \tilde{C}_m \lambda_m \boldsymbol{\Psi}_{3m} e^{-\mathrm{i}k_0 \lambda_m L} = \sum_{j=0}^{N_1} F_j \boldsymbol{\Phi}_{3j}, \tag{7}$$

$$\sum_{m=0}^{N_c} B_m \lambda_m \boldsymbol{\Psi}_{Sm} - \sum_{m=0}^{N_c} \tilde{C}_m \lambda_m \boldsymbol{\Psi}_{Sm} e^{-\mathrm{i}k_0 \lambda_m L} = \mathbf{0}, \tag{8}$$

$$\sum_{j=0}^{N_1} A_j \gamma_j \boldsymbol{\Phi}_{Sj} = \sum_{j=0}^{N_1} F_j \gamma_j \boldsymbol{\Phi}_{Sj}, \tag{9}$$

$$\sum_{m=0}^{N_c} B_m \boldsymbol{\Psi}_{3m} e^{-\mathrm{i}k_0 \lambda_m L} + \sum_{m=0}^{N_c} \tilde{C}_m \boldsymbol{\Psi}_{3m} - \sum_{n=0}^{N_1} D_n \boldsymbol{\Phi}_{3n} = \mathbf{0}, \tag{10}$$

$$\sum_{m=0}^{N_c} B_m \lambda_m \mathbf{\Psi}_{3m} e^{-\mathrm{i}k_0 \lambda_m L} - \sum_{m=0}^{N_c} \tilde{C}_m \lambda_m \mathbf{\Psi}_{3m} - \sum_{n=0}^{N_1} D_n \gamma_n \mathbf{\Phi}_{3n} = \mathbf{0}, \tag{11}$$

$$\sum_{m=0}^{N_c} B_m \lambda_m \mathbf{\Psi}_{Sm} e^{-\mathrm{i}k_0 \lambda_m L} - \sum_{m=0}^{N_c} \tilde{C}_m \lambda_m \mathbf{\Psi}_{Sm} = \mathbf{0}, \tag{12}$$

$$\sum_{n=0}^{N_1} D_n \gamma_n \mathbf{\Phi}_{Sn} = \mathbf{0}. \tag{13}$$

Here, $\tilde{C}_m = C_m e^{\mathrm{i}k_0 \lambda_m L}$, N_1 is the number of nodes in the finite element mesh in region R_1; N_c is the number of nodes in the silencer chamber ($N_c = N_2 + N_3 + N_4$). Vector $\mathbf{\Psi}_3$ holds those nodal values in the silencer that lie in the airway (R_2); vector $\mathbf{\Phi}_3$ holds those nodes in the inlet/outlet duct that lie on transverse locations identical to those chosen for $\mathbf{\Psi}_3$. Vector $\mathbf{\Psi}_S$ encompasses all nodes that lie in the porous material; $\mathbf{\Phi}_S$ contains all nodes in the inlet/outlet duct that lie adjacent to the splitter fairing. Equations (6) to (13) may be solved only after choosing appropriate amplitudes for F_j. Following references [4, 5, and 6], equal modal energy density (EMED) is chosen as this best represents the incident sound field propagating from a fan. Accordingly,

$$\left|F_j / p_0\right|^2 = I_0 \Big/ I_J \sum_{m=1}^{N_I} \gamma_m \text{, where } I_n = \int_0^{r_3} r \left|\Phi_n(r)\right|^2 dr \tag{14a, b}$$

and p_0 is a reference pressure chosen here, arbitrarily, to be equal to unity; N_I is the number of modes propagating in the inlet duct. A common method for representing silencer performance is transmission loss (TL), which may be written as [5]

$$TL = -10 \log_{10} \sum_{n=0}^{N_I} \frac{\gamma_n I_n \left|D_n\right|^2}{I_0}. \tag{15}$$

RESULTS AND DISCUSSION

Predictions are presented here for two different silencer geometries. The first (silencer A) has a geometry identical to a silencer studied by Munjal [3], and is excited by a plane wave. The second (silencer B) is chosen to be larger and is also excited by a multi-mode incident sound field. For both silencers, the absorbent material is fibrous and bulk reacting, so that the regression formulae of Delany and Bazley [7] may be used to specify the bulk acoustic properties (see also [5]). An expression for the impedance of the perforate is taken from Kirby [5].

In Fig. 1, transmission loss (TL) predictions are presented for silencer A ($r_1 = 0.05$ m, $r_2 = 0.1$ m, $r_3 = 0.15$ m, $L = 0.5$ m; $\sigma = 15000$ Pa s/m^2, where σ is the material flow resistivity). The TL predictions are compared in Fig. 1 with predictions for the attenuation (α) of the first and second propagating modes in the silencer, where $\alpha_n = -8.6858\, L\, \Im(k_0 \lambda_n)$, and with the plane wave predictions of Munjal [3]. The geometry of silencer A is identical to one of the silencers studied by Munjal apart for the inclusion of fairings in the current model, and the choice of perforate model. Munjal does not give a value for his perforate porosity (Ω), and so the value chosen here is that which provides the best fit between attenuation of the fundamental mode in the current model and the TL predictions of Munjal: this value is $\Omega = 0.135$. In Figure 1, the TL predictions of Munjal and the attenuation of the least attenuated mode agree well; however, it is noticeable here that the higher order modes in the silencer are highly attenuated and so one would expect the performance of the silencer to be dominated by the fundamental mode. Moreover, it is likely that the discrepancy between the multi-mode TL predictions and the fundamental mode is largely down to scattering of higher order modes at the fairings, although it is possible that higher order modes propagating within the silencer influence performance at higher frequencies. Note also that the peaks seen in the TL predictions are caused by higher order modes cutting on in the outlet duct.

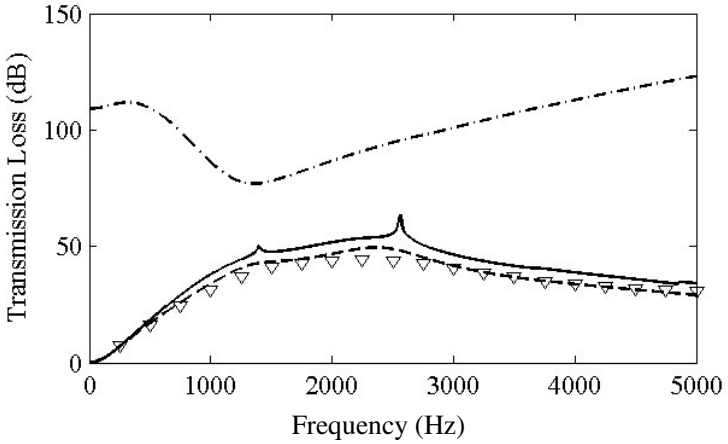

Figure 1. Predictions for silencer A: ——, TL multi-mode; — —, attenuation of mode 1; — - —, attenuation of mode 2; ∇, data of Munjal [3].

The silencer studied by Munjal contains a material with a very high flow resistivity. Such high values may be encountered in automotive exhaust silencers, but are rarely found in HVAC systems; instead, flow resistivity values normally range from, say, 3000 to 7000 Pa s/m^2. In Fig. 2 TL predictions are presented for the plane wave excitation of silencer A, but with a modified flow resistivity of $\sigma = 7000$ Pa s/m^2. It is evident in Fig. 2 that the higher order modes are now far less attenuated, and that the second and third modes significantly affect silencer performance, even for this relatively small silencer. The predictions in Fig. 2 caution against assuming plane wave propagation in pod silencers used in HVAC applications.

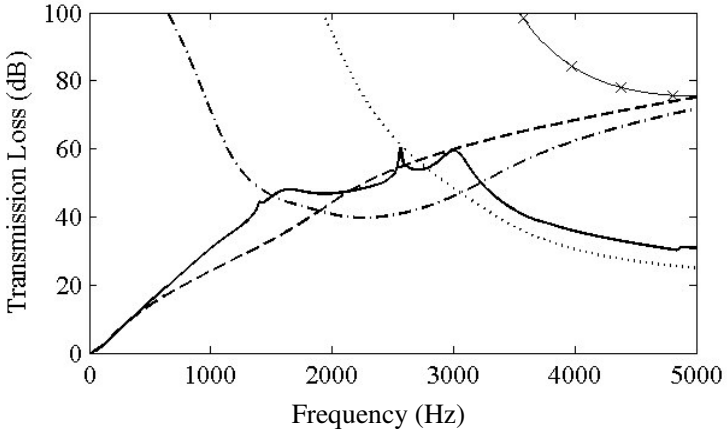

Figure 2. Predictions for silencer A: ——, TL multi-mode; — —, attenuation of mode 1; — - —, attenuation of mode 2;- - - -, attenuation of mode 3; —×—, attenuation of mode 4.

In Figs 3 and 4 predictions are shown for silencer B, which is larger than silencer A ($r_1 = 0.25$ m , $r_2 = 0.5$ m , $r_3 = 0.75$ m , $L = 2$ m , $\sigma = 7000$ Pa s/m^2 , and $\Omega = 0.33$). In Fig. 3, a plane wave sound field excites the silencer and it is seen that the TL drops significantly at higher frequencies as sound energy "beams" down the (larger) airway. What is noticeable in Fig. 3 is the relatively small effect of the higher order modes on silencer TL, although this is probably just a function of the silencer geometry chosen and cannot be relied upon as a general design guide.

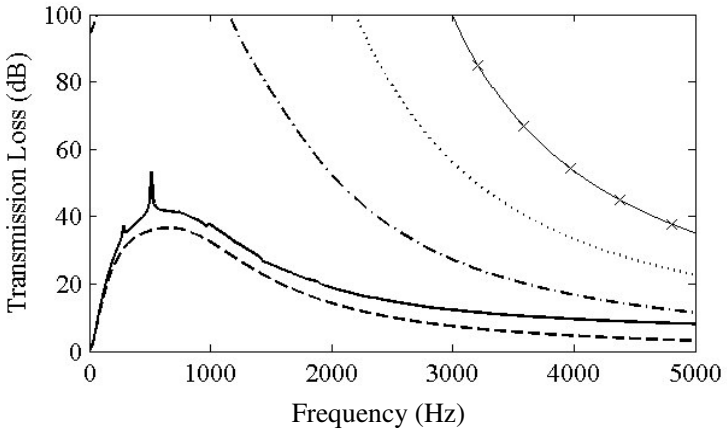

Figure 3. Silencer B (plane wave excitation): ——, TL;— —, attenuation of mode 1; — - —, attenuation of mode 2; - - - -, attenuation of mode 3; —×—, attenuation of mode 4.

In Fig. 4, silencer B is excited by a multi-mode sound field (EMED), a situation that better represents the actual conditions experienced by a pod silencer. It is evident here that as incident sound energy is transferred into higher order modes the TL increases at higher frequencies. Thus, at higher frequencies this type of silencer is more effective at attenuating higher order incident modes. Furthermore, the discrepancy between TL and the attenuation of the fundamental mode demonstrates

that, in order to model performance in a real system, it is necessary to account for all modes propagating in both the silencer and the inlet/outlet ducts.

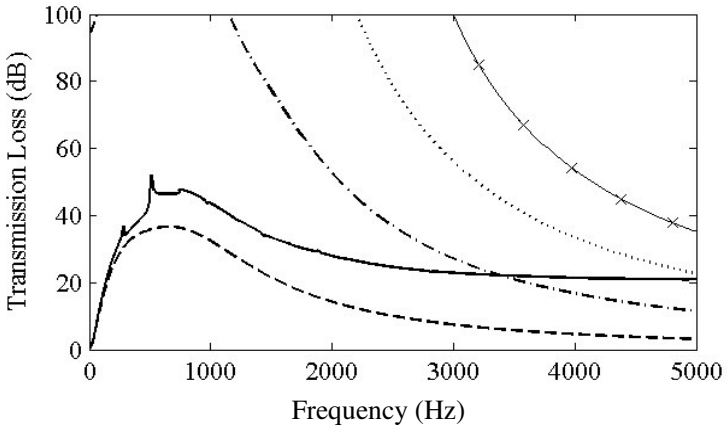

Figure 4. Silencer B (EMED excitation): ——, TL;— —, attenuation of mode 1; — - —, attenuation of mode 2; - - - -, attenuation of mode 3; —×—, attenuation of mode 4.

CONCLUSIONS

The point collocation technique has been applied here to pod silencers of the type typically found in HVAC applications. Transmission loss predictions are presented for two different silencers and, after comparison with modal attenuation rates, it is shown that higher order modes significantly influence silencer performance, even for relatively small silencers. Moreover, if multi-mode incident sound waves are present (as is likely downstream of a fan) then silencer performance is significantly different to that found under plane wave conditions. This places a question mark over how accurately those transmission loss measurements taken under plane wave conditions replicate the performance of silencers under real operating conditions.

REFERENCES

[1] Astley R.J., Cummings A., "A finite element scheme for attenuation in ducts lined with porous material: comparison with experiment", J. Sound. Vib., **116**, 239-263 (1987).

[2] Cummings A., Sormaz N., "Acoustic attenuation in dissipative splitter silencers containing mean fluid flow", J. Sound. Vib., **168**, 209-227 (1993).

[3] Munjal M.L., "Analysis and design of pod silencers", J. Sound. Vib., **262**, 497-507 (2003).

[4] Kirby R., Lawrie J.B., "A point collocation approach to modelling large dissipative silencers", J. Sound. Vib., **286**, 313-339 (2005).

[5] Kirby R., "The influence of baffle fairings on the acoustic performance of rectangular splitter silencers", J. Acoust. Soc. Am., **118**, 2302-2312 (2005).

[6] Lawrie J.B., Kirby R., "Mode-matching without root-finding: application to a dissipative silencer", J. Acoust. Soc. Am., to appear (2006).

[7] Delany M.E., Bazley E.N., "Acoustical properties of fibrous materials", Appl. Acoust., 56, 101-125 (1999).